Polyhedron 29 (2010) 606–612

Contents lists available at ScienceDirect

Polyhedron

journal homepage: www.elsevier.com/locate/poly

The molecular structure of a 2-aryl-1,3,2-dioxaphospholane and its coordination behaviour towards platinum(II) species; molecular structures of four platinum(II) complexes

Keith B. Dillon, Andrés E. Goeta, Philippa K. Monks *, Helena J. Shepherd

Chemistry Department, Durham University, South Road, Durham DH1 3LE, UK

ARTICLE INFO

Article history:
Available online 26 July 2009

Keywords:
Phosphonite
Phospholane
Platinum(II) complexes
Molecular structures
Phosphorus NMR

ABSTRACT

The molecular structure of the 2-aryl-1,3,2-dioxaphospholane, 2,6-$(CF_3)_2$-C_6H_3-$P(OCH_2)_2$ (**1**), has been determined by single-crystal X-ray diffraction at 120 K. Its reactions with the platinum(II) dimers *trans*-$[PtCl(\mu\text{-}Cl)(PEt_3)]_2$, *trans*-$[PtCl(\mu\text{-}Cl)(PPh_2Me)]_2$, *trans*-$[PtCl(\mu\text{-}Cl)(PPhMe_2)]_2$ and *trans*-$[PtBr(\mu\text{-}Br)(PEt_3)]_2$ have been investigated using ^{31}P NMR solution-state spectroscopy. Monomeric *trans*- and *cis*-Pt(II) complexes were formed; the molecular structures of *cis*-$[PtCl_2(L)(PR_2R')]$ (R=R′=Et (**3**), R=Ph, R′=Me (**7**)), *cis*-$[PtBr_2L(PEt_3)]$ (**9**) and *cis*-$[PtCl_2L_2]$ (**10**), where L = 2,6-$(CF_3)_2$-C_6H_3-$P(OCH_2)_2$, have been ascertained at 120 K.

1. Introduction

Complexes containing chiral phosphonites have been shown to act as catalysts for asymmetric hydrogenation [1–7] and asymmetric hydroformylation reactions [8,9]. Some 2-aryl-1,3,2-dioxaphospholanes (cyclic phosphonites), including 2,6-$(CF_3)_2$-C_6H_3-$P(OCH_2)_2$, have previously been prepared as potential precursors, via pyrolysis reactions, for metaphosphate intermediates [10]. With the exception of this reaction, there have been no reported investigations into the reactivity or coordination properties of 2,6-$(CF_3)_2$-C_6H_3-$P(OCH_2)_2$. Contrastingly, the coordination behaviour of benzo-3-(2,4,6-tri-*tert*-butylphenyl)-1,3,2-dioxaphospholane has previously been studied [11]. A gold(I) complex was prepared, but attempts to synthesise Pt(II) complexes of this ligand were unsuccessful, probably due to the steric bulk around the P(III) centre. Furthermore few 1,3,2-dioxaphospholanes have been structurally characterised [12–19].

It was therefore of considerable interest to investigate the structure and coordination chemistry of 3-(2,6-*bis*-(trifluoromethyl)-phenyl)-1,3,2-dioxaphospholane, 2,6-$(CF_3)_2$-C_6H_3-$P(OCH_2)_2$, which could act as a sterically hindered and electron-poor ligand.

2. Results and discussion

The 2-aryl-1,3,2-dioxaphospholane, 2,6-$(CF_3)_2$-C_6H_3-$P(OCH_2)_2$ (**1**), was prepared as previously described in a two-step reaction of TMEDA, ^{n}BuLi and 1,3-*bis*-(trifluoromethyl)benzene with ethylene chlorophosphite [10]. The formation of **1** was confirmed using both $^{31}P\{^1H\}$ (septet, 158.2 ppm, $^4J_{P-F}$ = 35 Hz) and ^{19}F NMR spectroscopy (d, −55.5 ppm, $^4J_{F-P}$ = 35 Hz) [10]. Crystals suitable for an X-ray structure determination were obtained, and the molecular structure at 120 K is shown in Fig. 1, with selected bond distances and angles listed in Table 1.

2,6-$(CF_3)_2$-C_6H_3-$P(OCH_2)_2$, (**1**), crystallises in the orthorhombic space group *Pnma*. There is a mirror plane along the P1–C1 bond which bisects both the aromatic 6-membered and the 5-membered rings, while the 5-membered heterocycle adopts an envelope conformation.

A few cyclic organophosphites have previously been structurally characterised [12–19]. The P–O bond distances in these compounds range between 1.558(3) and 1.702(2) Å, in good agreement with 1.634(1) Å determined for **1** [12–19]. The P–C bond distances for the cyclic organophosphites vary between 1.790(5) and 1.9135(21) Å, depending on the nature of the substituent. Hence the P–C bond length in **1** (1.894(2) Å) is also similar to those previously reported [12–19].

2.1. Coordination properties

In order to investigate its coordination properties towards platinum(II), **1** was reacted separately in a 2:1 molar ratio with the dimeric complexes *trans*-$[PtCl(\mu\text{-}Cl)(PEt_3)]_2$, *trans*-$[PtCl(\mu\text{-}Cl)(PPhMe_2)]_2$, *trans*-$[PtCl(\mu\text{-}Cl)(PPh_2Me)]_2$ and *trans*-$[PtBr(\mu\text{-}Br)(PEt_3)]_2$ (Scheme 1). The reactions were followed by ^{31}P NMR solution-state spectroscopy. Monomeric platinum(II) complexes of the general formula $[PtX_2(L)(PR_2R')]$, where L = 2,6-$(CF_3)_2$-C_6H_3-$P(OCH_2)_2$, were formed as the major products in each case

* Corresponding author. Tel.: +44 (0)191 334 2084; fax: +44 (0)191 384 4737.
E-mail address: p.k.monks@durham.ac.uk (P.K. Monks).

0277-5387/$ - see front matter © 2009 Elsevier Ltd. All rights reserved.
doi:10.1016/j.poly.2009.07.040

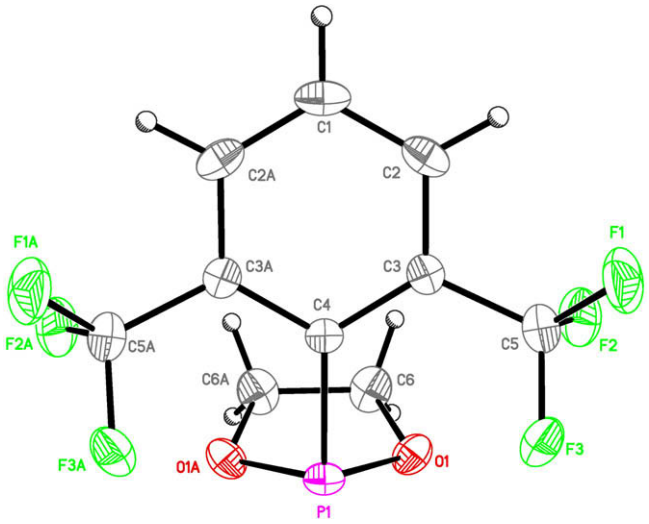

Fig. 1. The molecular structure of 2,6-$(CF_3)_2$-C_6H_3-$P(OCH_2)_2$ (**1**). Thermal ellipsoids are drawn at 50% probability.

(Scheme 1). Initially the *trans* isomers were formed as the kinetic products, and these converted slowly to the more thermodynamically stable *cis* isomers on standing. $^{31}P\{^1H\}$ NMR data for the complexes are shown in Table 2. In all instances where *trans*/*cis* pairs were formed, the *trans* isomer showed a much larger $^2J_{P-P}$ value and a relatively smaller $^1J_{Pt-P}$ value than the *cis* isomer, in accordance with literature data [20,21].

Table 1
Selected bond distances (Å) and bond angles (°) for 2,6-$(CF_3)_2$-C_6H_3-$P(OCH_2)_2$ (**1**).

Bond distances (Å)	
P(1)–O(1)	1.634(1)
P(1)–O(1A)	1.634(1)
P(1)–C(4)	1.894(2)
F(1)–C(5)	1.340 (2)
O(1)–C(6)	1.439(2)
C(1)–C(2)	1.382(2)
Bond angles (°)	
O(1)–P(1)–O(1A)	93.87(7)
O(1A)–P(1)–C(4)	98.41(5)
O(1)–P(1)–C(4)	98.41(5)

The reaction of **1** with *trans*-$[PtCl(\mu\text{-}Cl)(PEt_3)]_2$ initially showed formation of *trans*-$[PtCl_2(L)(PEt_3)]$ (**2**) which converted to the *cis* isomer **3** on standing. Yellow crystals of the *cis* isomer **3** suitable for X-ray diffraction studies were isolated. The molecular structure of **3** at 120 K is shown in Fig. 2, while selected bond distances and angles are listed in Table 3.

Reaction of **1** with *trans*-$[PtCl(\mu\text{-}Cl)(PPhMe_2)]_2$ afforded a *trans* complex, **4**, as indicated by the large $^2J_{P-P}$ (691 Hz) and small $^1J_{Pt-P}$ coupling constants (Table 2) [20,21]. Signals corresponding to two minor products of the reaction (<5%) were also observed in the $^{31}P\{^1H\}$ NMR spectrum. These were assigned to ligand scrambling products, *cis*-$[PtCl_2L_2]$ (**10**), where L = 2,6-$(CF_3)_2$-C_6H_3-$P(OCH_2)_2$, and *cis*-$[PtCl_2(PPhMe_2)_2]$ (**11**) (Fig. 3, Table 2). Upon standing **4** converted slowly to the more thermodynamically stable product, *cis*-$[PtCl_2(L)(PPhMe_2)]$ (**5**). The $^{31}P\{^1H\}$ NMR data for this complex are shown in Table 2. Attempts to obtain crystalline material of either **4** or **5** from the reaction mixture were unsuccessful.

By repeating the reaction of **1** with *trans*-$[PtCl(\mu\text{-}Cl)(PPhMe_2)]_2$, micro-crystalline material was isolated, but was unsuitable for analysis by X-ray diffraction. Gentle heating of the solution to redissolve this material appeared to promote ligand scrambling, and crystals of *cis*-$[PtCl_2L_2]$ (**10**), were isolated as the major product. The molecular structure of **10** was ascertained at 120 K, and its structure is shown in Fig. 4, with selected bond lengths and angles reported in Table 4. Although the ligand scrambling products were initially minor products in this reaction, exchange reactions of this type are known for similar Pt(II) complexes, where upon prolonged standing complete ligand exchange was found to occur [22]. Ligand scrambling has also been reported between two platinum complexes PtX_2L_2 and PtR_2L_2 (where X = halide/anionic ligand, R = aryl/alkyl and L = tertiary phosphine/arsine) to afford *cis*-$[PtXRL_2]$, which then converts to the *trans* isomer [23–25].

Reaction of **1** with *trans*-$[PtCl(\mu\text{-}Cl)(PPh_2Me)]_2$ initially afforded four platinum-containing complexes, including both the *trans* (10%) (**6**) and *cis* (50%) (**7**) complexes (Scheme 1). The $^{31}P\{^1H\}$ NMR data for these two complexes are shown in Table 2. The other

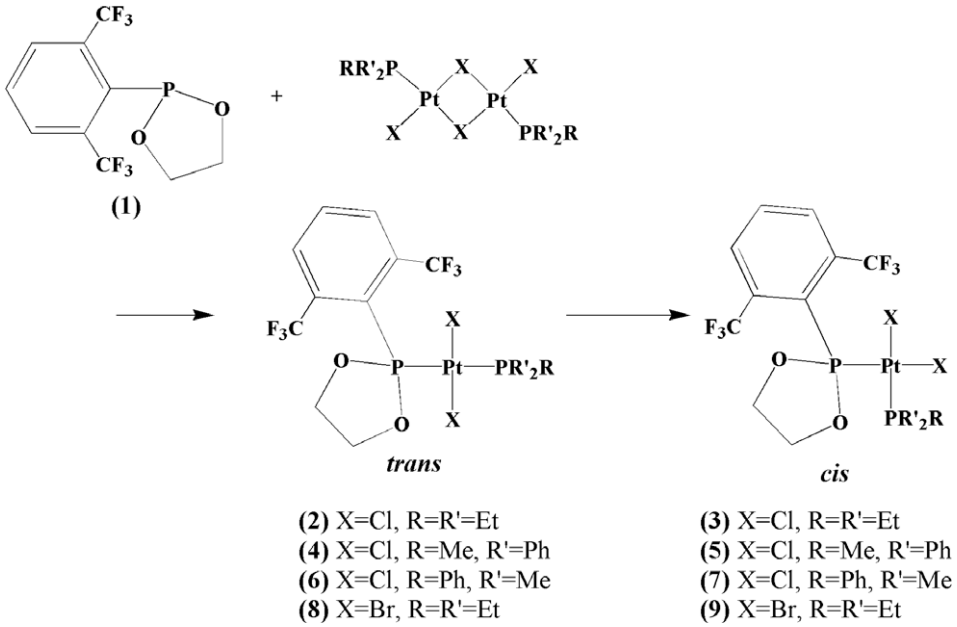

(2) X=Cl, R=R'=Et
(4) X=Cl, R=Me, R'=Ph
(6) X=Cl, R=Ph, R'=Me
(8) X=Br, R=R'=Et

(3) X=Cl, R=R'=Et
(5) X=Cl, R=Me, R'=Ph
(7) X=Cl, R=Ph, R'=Me
(9) X=Br, R=R'=Et

Scheme 1. Reaction of 2,6-$(CF_3)_2$-C_6H_3-$P(OCH_2)_2$ (**1**) with *trans*-$[PtX(\mu\text{-}X)(PR_2R')]_2$.

Table 2
^{31}P NMR data for complexes (**2**)–(**12**) (P_B corresponds to (L)).

Complex	δP_A, ppm	δP_B, ppm	$^1J_{Pt-PA}$, Hz	$^1J_{Pt-PB}$, Hz	$^2J_{PA-PB}$, Hz
trans-[$PtCl_2(L)(PEt_3)$] (**2**)	14.6	144.2	2521	3581	651
cis-[$PtCl_2(L)(PEt_3)$] (**3**)	18.8	115.5	3102	5670	21
trans-[$PtCl_2(L)(PPhMe_2)$] (**4**)	−6.9	142.5	2547	3681	691
cis-[$PtCl_2(L)(PPhMe_2)$] (**5**)	−9.4	113.0	3192	5573	23
trans-[$PtCl_2(L)(PPh_2Me)$] (**6**)	4.7	140.4	2594	3766	687
cis-[$PtCl_2(L)(PPh_2Me)$] (**7**)	1.1	111.7	3280	5538	21
trans-[$PtBr_2(L)(PEt_3)$] (**8**)	10.1	141.0	2441	3468	647
cis-[$PtBr_2(L)(PEt_3)$] (**9**)	18.4	112.4	3051	5591	17
cis-[$PtCl_2L_2$] (**10**)	–	114.1	–	5180	–
cis-[$PtCl_2(PPhMe_2)_2$] (**11**)	−21.8	–	3700	–	–
cis-[$PtCl_2L(PPh_2Me)_2$] (**12**)	0.1	–	3600	–	–

two complexes were assigned to the ligand scrambling products, *cis*-[$PtCl_2L_2$] (**10**) (s, 114.0 ppm, $^1J_{Pt-P}$ = 5180 Hz) and *cis*-[$PtCl_2(PPh_2Me)_2$] (**12**) (s, 0.1 ppm, $^1J_{Pt-P}$ = 3600 Hz), the data for the latter being in good agreement with those in the literature [26]. Crystals of **7** suitable for single-crystal X-ray diffraction studies were isolated; the resulting molecular structure is shown in Fig. 5, with selected bond lengths and angles in Table 3.

Reaction of **1** with *trans*-[$PtBr(\mu\text{-}Br)(PEt_3)]_2$ was carried out in order to synthesise a bromo analogue of **3** and **4**. Initially the *trans* complex, *trans*-[$PtBr_2(L)(PEt_3)$] (**8**) formed. However, as in previous reactions of **1** with other Pt(II) dimers, this converted to the *cis* isomer, *cis*-[$PtBr_2(L)(PEt_3)$] (**9**), upon standing. Crystals suitable for X-ray diffraction studies were obtained of **9**, with the resulting molecular structure being shown in Fig. 6; selected bond distances and angles are listed in Table 3.

For the *cis*-[$PtX_2(L)(PR_2R')$] complexes **3**, **7** and **9**, the geometry around the Pt centre is approximately square planar, with the angles around Pt varying from 85.66(3)° to 95.33(3)°, 85.91(2)° to 95.21(2)° and 86.07(3)° to 95.08(4)°, respectively, the larger P(1)–Pt(1)–P(2) angle to accommodate the bulk of the phosphane groups. The Pt(1)–P(2) bond lengths in **3** and **9** (2.264(1) Å and 2.276(1) Å, respectively) are similar in magnitude to those observed for other [$PtCl_2$(P1)(P2)] complexes where (P2) = PEt_3 (*e.g.* 2.264(2) and 2.261(2) Å in *cis*-[$PtCl_2(PEt_3)_2$] [27], 2.315(4) in *trans*-[$PtBr_2(PEt_3)_2$] [28], 2.298(18) in *trans*-[$PtCl_2(PEt_3)_2$] [28], or 2.305(6) Å in *cis*-[$PtCl_2(PCy_3)(PEt_3)$]) [29]. Similarly, the Pt(1)–P(2) bond length in (**7**) (2.262(1) Å) is comparable to those ob-

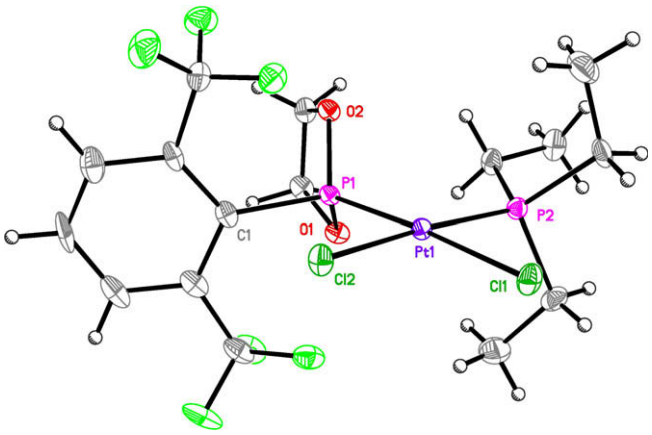

Fig. 2. The molecular structure of *cis*-[$PtCl_2(L)(PEt_3)$] (**3**), showing the numbering scheme for the key atoms. Thermal ellipsoids are drawn at 50% probability.

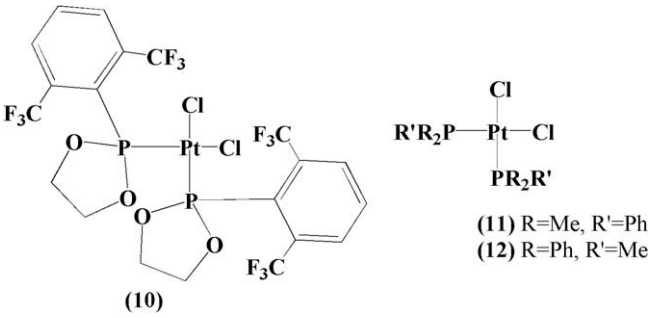

Fig. 3. Ligand scrambling products.

Table 3
Selected bond distances (Å) and bond angles (°) for (**3**), (**7**) and (**9**).

	cis-[$PtCl_2(L)(PEt_3)$] (**3**) (X=Cl)	*cis*-[$PtCl_2(L)(PPh_2Me)$] (**7**) (X=Cl)	*cis*-[$PtBr_2(L)(PEt_3)$] (**9**) (X=Br)
Bond distances (Å)			
Pt(1)–P(1)	2.183(1)	2.189(1)	2.192(1)
Pt(1)–P(2)	2.264(1)	2.262(1)	2.276(1)
Pt(1)–X(1)	2.356(1)	2.337(1)	2.487(1)
Pt(1)–X(2)	2.353 (1)	2.361 (1)	2.483 (1)
P(1)–C(1)	1.851(4)	1.856(2)	1.845(5)
P(1)–O(1)	1.603(2)	1.601(2)	1.603(3)
P(1)–O(2)	1.598(3)	1.600 (2)	1.603(3)
Bond angles (°)			
P(1)–Pt(1)–P(2)	95.33(3)	95.21(2)	95.08(4)
P(1)–Pt(1)–X(2)	90.12(3)	91.46(2)	90.32(3)
P(2)–Pt(1)–X(1)	85.66(3)	85.91(2)	86.07(3)
X(1)–Pt(1)–X(2)	88.82(3)	87.27(2)	88.54(2)
O(1)–P(1)–O(2)	96.81(13)	96.87(8)	96.82(17)
O(1)–P(1)–C(1)	100.79(15)	101.75(9)	100.5(2)
O(2)–P(1)–C(1)	102.91(15)	103.88(9)	102.91(19)

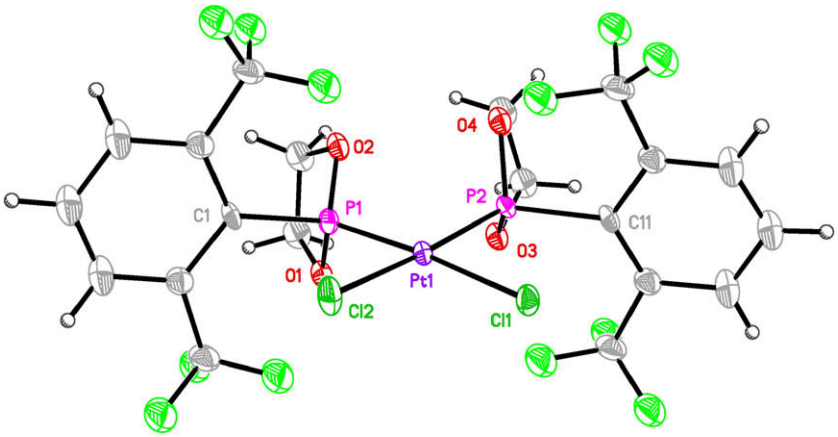

Fig. 4. The molecular structure of *cis*-[$PtCl_2L_2$] (**10**), showing the numbering scheme for the key atoms. Thermal ellipsoids are drawn at 50% probability.

Table 4
Selected bond distances (Å) and bond angles (°) for *cis*-[$PtCl_2L_2$] (**10**).

Bond distances (Å)	
Pt(1)–P(1)	2.206(4)
Pt(1)–P(2)	2.204(4)
Pt(1)–Cl(1)	2.337(4)
Pt(1)–Cl(2)	2.349(4)
P(1)–C(1)	1.823(13)
P(1)–O(1)	1.587(9)
P(1)–O(2)	1.591(11)
P(2)–C(11)	1.874(14)
P(2)–O(3)	1.577(10)
P(2)–O(4)	1.584(10)
Bond angles (°)	
P(1)–Pt(1)–P(2)	91.77(14)
P(2)–Pt(1)–Cl(1)	90.59(12)
P(1)–Pt(1)–Cl(2)	90.87(13)
Cl(1)–Pt(1)–Cl(2)	87.15(13)
O(1)–P(1)–O(2)	97.6(5)
O(3)–P(2)–O(4)	97.4(5)
O(1)–P(1)–C(1)	104.2(6)
O(2)–P(1)–C(1)	103.8(6)
O(3)–P(2)–C(11)	103.2(6)
O(4)–P(2)–C(11)	103.2(6)

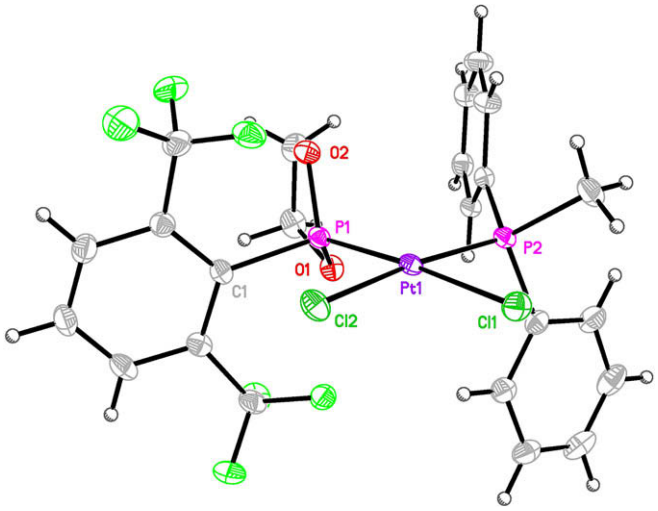

Fig. 5. The molecular structure of *cis*-[$PtCl_2(L)(PPh_2Me)$] (**7**), showing the numbering scheme for the key atoms. Thermal ellipsoids are drawn at 50% probability.

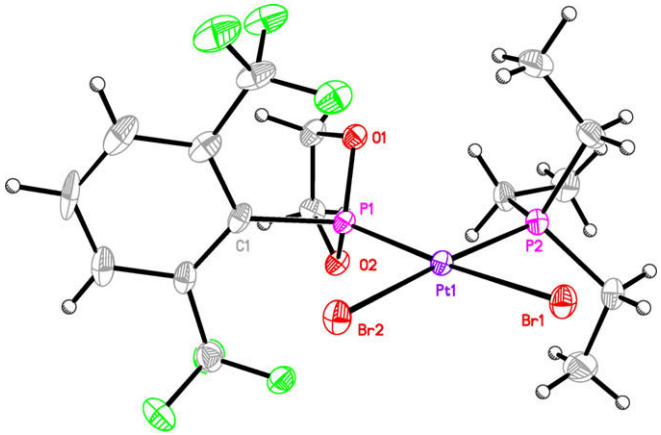

Fig. 6. The molecular structure of *cis*-[$PtBr_2(L)(PEt_3)$] (**9**), showing the numbering scheme for the key atoms. Thermal ellipsoids are drawn at 50% probability.

served for other [$PtClX(PPh_2Me)_2$] complexes that range between 2.239(2) and 2.3589(9) Å [30–34]. However, the Pt(1)–P(1) bond length for each complex is much shorter (2.183(1) Å (**3**), 2.189(1) (**7**) and 2.192(1) (**9**)), which is consistent with the larger $^1J_{Pt-P(1)}$ coupling constant observed for these three complexes (Table 2) [35–37]. This stronger bond probably arises from the more electronegative nature of the 2-aryl-1,3,2-dioxaphospholane ligand.

The complex *cis*-[$PtCl_2L_2$] (**10**), crystallises in the orthorhombic space group $P2_12_12_1$. The geometry around the Pt centre is approximately square planar, with the angles around Pt varying from 87.15(13)° to 91.77(14)°, the larger angle being the P(1)–Pt(1)–P(2) angle to accommodate the bulk of the phosphane groups. The Pt–P distances (2.206(4) and 2.204(4) Å) are slightly longer than those observed in complexes (**3**), (**7**) and (**9**) (2.183(1), 2.189(1) and 2.192(1) Å, respectively), and the P(1)–Pt(1)–P(2) angle is smaller at 91.77(13)°.

In **1** the O(1)–C(6)–C(6A)–O(1A) torsion angle is 0° as a consequence of the symmetry imposed by the mirror plane, which bisects the two carbon atoms in the 5-membered ring. There are no intermolecular short contacts present between the components of the 5-membered ring and any other part of the molecule, although there are intramolecular interactions between C6–H6A···F2′, and C6–H6B···C2′ of adjacent molecules. The angle between the planes defined by O–P–O and that of the O–C–C–O of the 5-membered ring ('envelope' angle) in **1** is 26°.

There are also no intermolecular interactions between the 5-membered ring and any other part of the molecule in complexes **3**, **7**, **9** and **10**. Complexes **3** and **9** are isostructural, with similar intermolecular interactions involving the dioxaphospholane moiety. One of the two ligands in **10** also shares a similar network of intermolecular short contacts; the envelope angles in these complexes are comparable to that observed in **1** – approximately 27° in all three complexes.

In complex **7** and the second dioxaphospholane ligand in **10**, the intramolecular interactions differ, resulting in a significant change in the 'envelope' angle, to approximately 20°. In addition to the change in this angle, there are considerable differences in the O–C–C–O torsion angle in these instances where the non-bonding interactions differ. These observations suggest that the geometry of the 5-membered ring is largely a result of intramolecular interactions.

Complexation of **1** results in a decrease in the P–O bond lengths in each case, and a widening of the O–P–O and O–P–C bond angles (Tables 1, 3 and 4). This is entirely in keeping with complexation via the lone pair on P to Pt, reducing the repulsion from the lone pair to the bonding pairs around the phosphorus centre. The P–C distance is also slightly reduced in **3**, **7** and **10**, although it is slightly larger in the *trans* complex **9**, possibly arising from greater steric interactions. The Pt–P distances are also slightly larger in **9** than in **3** or **7**. It is also of interest to note that the non-bonding O–O distances in **1**, and the four complexes **3**, **7**, **9** and **10** are very similar (2.380(10)–2.398(4) Å). This parallels the findings by Gillespie in, for example, BF_n and CF_n groups, where the F···F interligand distances are remarkably constant, despite variation in both bond distance and bond angle [38]. This again shows the importance of non-bonding interactions in influencing the structures of compounds.

Several similar Pt(II) complexes containing organophosphonite ligands and two chlorides have been previously structurally characterised [1,8,9,39–42]. The P–O bond lengths in these complexes range from 1.565(7) to 1.622(6) Å [1,8,9,39–42]. This is in good agreement with those found in complexes **3**, **7**, **9** and **10** (Tables 3 and 4). However, a search of the Cambridge Structural Database revealed no pairs of a structurally characterised dioxyphospholane, and its platinum complexes, therefore no comparison can be made of the changes to bond distances and angles of the ligands upon complexation [43].

3. Conclusions

Using single-crystal X-ray diffraction studies, the molecular structure of 2,6-$(CF_3)_2$-C_6H_3-$P(OCH_2)_2$ (**1**) has been ascertained at 120 K. The coordination behaviour of this phosphane towards some Pt(II) dimers has been investigated, resulting in the synthesis of the first transition metal complexes of 2,6-$(CF_3)_2$-C_6H_3-$P(OCH_2)_2$, which have been characterised using $^{31}P\{^1H\}$ NMR spectroscopy and single-crystal X-ray diffraction.

For each reaction of **1** with the platinum(II) dimers *trans*-$[PtCl(\mu\text{-}Cl)(PEt_3)]_2$, $[PtCl(\mu\text{-}Cl)(PPh_2Me)]_2$, $[PtCl(\mu\text{-}Cl)(PPhMe_2)]_2$ and $[PtBr(\mu\text{-}Br)(PEt_3)]_2$, monomeric Pt(II) complexes ($[PtX_2(L)(PR_2R')]$) were formed. The *trans* isomer formed initially as the kinetic product of the reaction, but over time this converted to the more thermodynamically stable *cis* isomer. For each reaction, the chemical shift of the chlorophosphane ligand of the *trans* complex was always to higher frequency than for the *cis*. For the *cis* complexes, large values of $^1J_{Pt-P}$ were observed (3051–5670 Hz) along with small values of $^2J_{P-P}$ (17–23 Hz) compared with the *trans* complexes, where the $^2J_{P-P}$ values are much larger (647–691 Hz) and $^1J_{Pt-P}$ values are much smaller (2441–3766 Hz). This is comparable with the data reported by Pidcock et al. [20] and Grim et al. [21] for other Pt(II) complexes.

For reactions of **1** with *trans*-$[PtCl(\mu\text{-}Cl)(PPhMe_2)]_2$ and with *trans*-$[PtCl(\mu\text{-}Cl)(PPh_2Me)]_2$, ligand scrambling products were observed as a minor component of the crude reaction mixtures. In

Table 5
Experimental data from crystallographic studies of compounds (**1**), (**3**), (**7**), (**9**) and (**10**).

Identification code	(**1**)	(**3**)	(**7**)	(**9**)	(**10**)
Complex	L	*cis*-$[PtCl_2(L)(PEt_3)]$	*cis*-$[PtCl_2(L)(PPh_2Me)]$	*cis*-$[PtBr_2(L)(PEt_3)]$	*cis*-$[PtCl_2L_2]$
Empirical formula	$C_{10}H_7F_6O_2P$	$C_{16}H_{22}Cl_2F_6O_2P_2Pt$	$C_{23}H_{20}Cl_2F_6O_2P_2Pt$	$C_{16}H_{22}Br_2F_6O_2P_2Pt$	$C_{21}H_{15}Cl_5F_{12}O_4P_2Pt$
Formula weight	304.12	688.27	770.32	777.19	993.61
Temperature	120(2)	120(2)	120(2)	120(2)	120(2)
Crystal system	orthorhombic	monoclinic	monoclinic	monoclinic	orthorhombic
Space group	*Pnma*	*Pn*	$P2_1/c$	*Pn*	$P2_12_12_1$
a (Å)	9.1335(6)	8.6707(6)	14.1043(7)	8.9108(4)	13.1502(16)
b (Å)	9.8055(6)	12.5959(9)	12.8346(7)	12.5588(5)	13.9552(17)
c (Å)	12.9490(8)	10.0326(7)	15.1574(8)	10.1267(4)	16.580(2)
β (°)		90.814(1)	110.943(1)	90.587(1)	
V (Å^3)	1159.69(13)	1095.60(13)	2562.6(2)	1133.21(8)	3042.7(6)
Z	4	2	4	2	4
D_{calc} (mg/mm^3)	1.742	2.086	1.997	2.278	2.169
m/mm^{-1}	0.312	6.854	5.873	9.917	5.260
F(0 0 0)	608	660	1480	732	1896
Crystal size (mm)	0.19 × 0.17 × 0.16	0.19 × 0.16 × 0.11	0.25 × 0.21 × 0.2	0.21 × 0.17 × 0.11	0.17 × 0.14 × 0.13
θ Range for data collection	2.61–28.35°	1.62–28.33°	1.55–26.37°	1.62–25.02°	1.91–25.02°
Index ranges	$-12 \leqslant h \leqslant 12$	$-11 \leqslant h \leqslant 11$	$-17 \leqslant h \leqslant 17$	$-10 \leqslant h \leqslant 10$	$-14 \leqslant h \leqslant 15$
	$-13 \leqslant k \leqslant 11$	$-16 \leqslant k \leqslant 16$	$-16 \leqslant k \leqslant 16$	$-13 \leqslant k \leqslant 14$	$-16 \leqslant k \leqslant 15$
	$-15 \leqslant l \leqslant 17$	$-13 \leqslant l \leqslant 13$	$-18 \leqslant l \leqslant 18$	$-7 \leqslant l \leqslant 12$	$-19 \leqslant l \leqslant 19$
Reflections collected	10638	16293	31919	6309	16480
Independent reflections	1519 [R_{int} = 0.0268]	5351 [R_{int} = 0.0317]	5234 [R_{int} = 0.0217]	3327 [R_{int} = 0.0221]	5375 [R_{int} = 0.0970]
Data/restraints/parameters	1519/0/106	5351/2/265	5234/0/326	3327/2/265	5375/0/232
Goodness-of-fit (GOF) on F^2	1.068	0.823	1.045	0.935	1.014
Final *R* indexes [$I > 2\sigma(I)$]	R_1 = 0.0296	R_1 = 0.0184	R_1 = 0.0147	R_1 = 0.0180	R_1 = 0.0551
	wR_2 = 0.0761	wR_2 = 0.0394	wR_2 = 0.0360	wR_2 = 0.0382	wR_2 = 0.1150
Final *R* indexes [all data]	R_1 = 0.0343	R_1 = 0.0200	R_1 = 0.0166	R_1 = 0.0185	R_1 = 0.0962
	wR_2 = 0.0790	wR_2 = 0.0400	wR_2 = 0.0372	wR_2 = 0.0384	wR_2 = 0.1322
Largest differential in peak/hole	0.397/−0.281	0.914/−0.419	1.173/−0.636	0.907/−0.588	2.610/−2.683
Flack parameter		0.021(4)		0.019(5)	0.030(13)

both reactions *cis*-[$PtCl_2L_2$], where L = 2,6-$(CF_3)_2$-C_6H_3-$P(OCH_2)_2$, (**10**) was observed, along with the corresponding *cis*-[$PtCl_2(PR_2R')_2$] complex (R=Me, R′=Ph (**11**) and R=Ph, R′=Me (**12**)). Crystals of the *bis*-(2,6-$(CF_3)_2$-C_6H_3-$P(OCH_2)_2$) ligand scrambling product **10** were isolated after heating the reaction of **1** with *trans*-[PtCl(μ-Cl)$(PPhMe_2)]_2$, and its structure was confirmed by single-crystal X-ray diffraction at 120 K.

Further studies on the reactivity and applications of these interesting systems are currently in progress.

4. Experimental

All manipulations, including NMR sample preparation, were carried out either under an inert atmosphere of dry nitrogen or *in vacuo*, using standard Schlenk line or glovebox techniques. Chemicals of the best available commercial grade were used, in general without further purification. The ^{31}P NMR spectra of all phosphorus-containing starting materials were recorded, to verify that no major impurities were present. ^{31}P NMR spectra were obtained on Varian Unity 300, Mercury 400 or Inova 500 Fourier-transform spectrometers at 121.40, 161.91 or 202.3 MHz, respectively; chemical shifts are referenced to 85% H_3PO_4, with the high frequency direction taken as positive. Microanalyses were performed by the microanalytical services of the Department of Chemistry, Durham University.

4.1. Synthesis of trans-[PtCl(μ-Cl)$(PEt_3)]_2$

$PtCl_2$ (4.53 g, 17.1 mmol) and PEt_3 (2.4 mL, 16.0 mmol) were added to *p*-chlorotoluene (15 mL) and the mixture was heated at reflux for 120 min [44]. The solvent was then removed *in vacuo* to afford a dark brown solid. CH_2Cl_2 (20 mL) was then added and the solution was filtered through Celite. The solid was washed with further quantities of DCM until the filtrate ran clear. Upon standing overnight, bright orange crystals formed. These were recrystallised from CH_2Cl_2. Yield = 10.56 g (80%) ($C_{12}H_{30}Cl_4P_2Pt_2$ requires C, 18.76; H, 3.94; N, 0.00. Found: C, 18.89; H, 3.95; N, 0.00%). ^{31}P (121.40 MHz, $CDCl_3$): δ 11.5 ppm (s, $^1J_{Pt-P}$ = 3839 Hz) (literature data: δ 9.78 ppm (s, $^1J_{Pt-P}$ = 3845 Hz) [44]).

4.2. Synthesis of trans-[PtCl(μ-Cl)$(PPh_2Me)]_2$

$PtCl_2$ (2.11 g, 7.96 mmol) and PPh_2Me (1.4 mL, 7.41 mmol) were added to *p*-chlorotoluene (10 mL) and the mixture was then heated to reflux for 90 min. The solvent was removed *in vacuo* to afford a dark brown solid. CH_2Cl_2 (20 mL) was then added and the solution was filtered through Celite. The solid was washed with further quantities of CH_2Cl_2 until the filtrate ran clear. The yellow filtrate was then concentrated to approximately 10 mL and pentane (40 mL) added, which resulted in the formation of a yellow precipitate. The solution was removed by filtration to leave the yellow solid. Yield = 6.12 g (82%) ($C_{26}H_{26}Cl_4P_2Pt_2$ requires C, 33.49; H, 2.81; N, 0.00. Found: C, 33.19; H, 2.87; N, 0.00%). ^{31}P (121.40 MHz, $CDCl_3$): δ −6.4 ppm (s, $^1J_{Pt-P}$ = 4003 Hz) (literature data: δ −4.2 ppm (s, $^1J_{Pt-P}$ = 3911 Hz) [45]).

4.3. Synthesis of trans-[PtCl(μ-Cl)$(PPhMe_2)]_2$

$PtCl_2$ (2.1 g, 7.96 mmol) and $PPhMe_2$ (1.4 mL, 7.41 mmol) were added to *p*-chlorotoluene (10 mL) and the mixture was heated at reflux for 90 min [44]. The solvent was removed *in vacuo* to afford a dark brown solid. CH_2Cl_2 (30 mL) was then added and the solution was filtered through Celite. The solid was washed with further quantities of CH_2Cl_2 until the filtrate ran clear. The filtrate was concentrated to approximately 10 mL and pentane (40 mL) added, causing the formation of a yellow precipitate. The solution was filtered to isolate the yellow solid. Yield = 4.93 g (77%) ($C_{16}H_{22}Cl_4P_2Pt_2$ requires C, 23.78; H, 2.74; N, 0.00. Found: C, 23.76; H, 2.75; N, 0.00%). ^{31}P (121.40 MHz, $CDCl_3$): δ −17.0 ppm (s, $^1J_{Pt-P}$ = 3928 Hz) (literature data: δ −18.5 ppm (s, $^1J_{Pt-P}$ = 3930 Hz) [44], δ −18.7 ppm (s, $^1J_{Pt-P}$ = 3934 Hz) [45]).

4.4. Synthesis of trans-[PtBr(μ-Br)$(PEt_3)]_2$

$PtBr_2$ (3.2860 g, 9.26 mmol) and PEt_3 (1.33 mL, 9.01 mmol) were added to *p*-chlorotoluene (20 mL) and the mixture was heated at reflux for 150 min. The solvent was then removed *in vacuo* to afford a dark brown solid. CH_2Cl_2 (20 mL) was then added and the solution was filtered through Celite. The solid was washed with further quantities of CH_2Cl_2 until the filtrate ran clear. Upon standing overnight bright orange crystals formed which were recrystallised from DCM. Yield = 6.40 g (73%). ($C_{12}H_{30}Br_4P_2Pt_2$ requires C, 15.23; H, 3.20; N, 0.00. Found: C, 15.10; H, 3.07; N, 0.00%). ^{31}P (161.9 MHz, $CDCl_3$): δ 11.0 ppm (s, $^1J_{Pt-P}$ = 3696 Hz) (literature data: δ 10.9 ppm (s, $^1J_{Pt-P}$ = 3701 Hz) [46]).

4.5. Synthesis of 2,6-$(CF_3)_2$-C_6H_3-$P(OCH_2)_2$

A solution of ethylene chlorophosphite (6.3 g, 50 mmol) in diethylether (50 mL) was prepared [10]. TMEDA (5.69 g, 49 mmol) and a solution of *n*-butyllithium (1.6 M in hexanes, 29.2 mL) were added to a solution of 1,3-*bis*-(trifluoromethyl)benzene (10.0 g, 46.7 mmol) in hexane (30 mL) at 0 °C. The solution was stirred overnight at room temperature. The solution was then added dropwise to the ethylene chlorophosphite solution. The resulting solution was filtered to remove lithium salts and the solvents were removed *in vacuo*. Upon standing colourless crystals were obtained. Yield 8.2 g (54%) ($C_{10}H_7F_6O_2P$ requires C, 39.49; H, 2.32; N, 0.00. Found: C, 39.09; H, 2.61; N, 0.00%). $^{31}P\{^1H\}$ ($CDCl_3$, 161.9 MHz): δ 158.2 ppm (septet, $^4J_{P-F}$ = 35 Hz); ^{19}F ($CDCl_3$, 376 MHz): −55.5 ppm (d, $^4J_{F-P}$ = 35 Hz). (literature data: ^{31}P (septet, 158.2 ppm, $^4J_{P-F}$ = 35 Hz);^{19}F (d, −55.5 ppm, $^4J_{F-P}$ = 35 Hz) [10]).

4.6. Synthesis of trans- and cis-$[PtCl_2(L)(PEt_3)]$, where L = 2,6-$(CF_3)_2$-C_6H_3-$P(OCH_2)_2$

A solution was prepared containing *trans*-[PtCl(μ-Cl)$(PEt_3)]_2$ (0.0253 g, 0.033 mmol) in $CDCl_3$ (1 mL). This solution was added to 2,6-$(CF_3)_2$-C_6H_3-$P(OCH_2)_2$ (0.0202 g, 0.066 mmol). A ^{31}P NMR spectrum was recorded soon after this addition. Slow evaporation of the solvent afforded crystalline material suitable for X-ray analysis. ($C_{16}H_{22}Cl_2F_6O_2P_2Pt$ requires C, 27.92; H, 3.22; N, 0.00. Found: C, 27.54; H, 3.39; N, 0.00%).

4.7. Synthesis of trans- and cis-$[PtCl_2(L)(PPhMe_2)]$, where L = 2,6-$(CF_3)_2$-C_6H_3-$P(OCH_2)_2$

A solution was prepared containing *trans*-[PtCl(μ-Cl)$(PPhMe_2)]_2$ (0.0323 g, 0.04 mmol) in $CDCl_3$ (1 mL). This solution was added to 2,6-$(CF_3)_2$-C_6H_3-$P(OCH_2)_2$ (0.0240 g, 0.08 mmol). A ^{31}P NMR spectrum was recorded soon after this addition.

4.8. Synthesis of trans- and cis-$[PtCl_2(L)(PPh_2Me)]$, where L = 2,6-$(CF_3)_2$-C_6H_3-$P(OCH_2)_2$

A solution was prepared containing *trans*-[PtCl(μ-Cl)$(PPh_2Me)]_2$ (0.0606 g, 0.075 mmol) in $CDCl_3$ (1 mL). This solution was then added to 2,6-$(CF_3)_2$-C_6H_3-$P(OCH_2)_2$ (0.0454 g, 0.15 mmol). A ^{31}P NMR spectrum was recorded soon after this addition. Slow evapo-

ration of the solvent afforded crystalline material suitable for X-ray analysis.

4.9. Synthesis of trans- and cis-[$PtBr_2(L)(PEt_3)$], where L = 2,6-$(CF_3)_2$-C_6H_3-$P(OCH_2)_2$

A solution was prepared containing *trans*-[$PtBr(\mu\text{-}Br)(PEt_3)]_2$ (0.0567 g, 0.06 mmol) in $CDCl_3$ (1 mL). This solution was then added to 2,6-$(CF_3)_2$-C_6H_3-$P(OCH_2)_2$ (0.0380 g, 0.12 mmol). A ^{31}P NMR spectrum was recorded soon after this addition. Slow evaporation of the solvent afforded crystalline material suitable for X-ray analysis. ($C_{16}H_{22}Br_2F_6O_2P_2Pt$ requires C, 24.73; H, 2.85; N, 0.00. Found: C, 24.82; H, 2.87; N, 0.00%).

4.10. Synthesis of cis-[$PtCl_2L_2$], where L = 2,6-$(CF_3)_2$-C_6H_3-$P(OCH_2)_2$

A solution was prepared containing *trans*-[$PtCl(\mu\text{-}Cl)(PPhMe_2)]_2$ (0.0606 g, 0.075 mmol) in $CDCl_3$ (1 mL). This solution was then added to 2,6-$(CF_3)_2$-C_6H_3-$P(OCH_2)_2$ (0.0454 g, 0.15 mmol). A ^{31}P NMR spectrum was recorded soon after this addition. Slow evaporation of the solvent afforded micro-crystalline material unsuitable for X-ray analysis. The solution was heated to redissolve the microcrystalline material, and a second ^{31}P NMR spectrum showed the formation of ligand scrambling products, *cis*-[$PtCl_2L_2$], where L = 2,6-$(CF_3)_2$-C_6H_3-$P(OCH_2)_2$ and *cis*-[$PtCl_2(PPhMe_2)_2$]. Slow evaporation of the solvent afforded crystalline material suitable for X-ray analysis, which proved to be *cis*-[$PtCl_2L_2$]. ($C_{20}H_{14}Cl_2F_{12}O_4P_2Pt$ requires C, 27.48; H, 1.61; N, 0.00 Found: C, 27.54; H, 1.63; N, 0.00%).

4.11. X-ray crystallography

Single-crystal structure determinations were carried out from data collected using graphite monochromated Mo Kα radiation (λ = 0.71073 Å) on a Bruker SMART-CCD 1 K diffractometer at 120 K. The temperature was controlled using a Cryostream N_2 flow cooling device [47]. In each case, a series of narrow ω-scans (0.3°) were performed at several φ-settings in such a way as to cover a sphere of data to a maximum resolution of 0.70 Å. Cell parameters were determined and refined using the SMART software [48], and raw frame data were integrated using the SAINT program [49]. The structures were solved and refined using OLEX2 [50] as an interface to SHELXS-97 and SHELXL-97 [51]. Crystal data are given in Table 5.

Supplementary data

CCDC 729917, 729918, 729919, 729920 and 729921 contains the supplementary crystallographic data for (**1**), (**3**), (**7**), (**9**) and (**10**). These data can be obtained free of charge via http://www.ccdc.cam.ac.uk/conts/retrieving.html, or from the Cambridge Crystallographic Data Centre, 12 Union Road, Cambridge CB2 1EZ, UK; fax: (+44) 1223-336-033; or e-mail: deposit@ccdc.cam.ac.uk.

Acknowledgements

We would like to thank the EPSRC for a research studentship (to HJS), the Maria da Graça Memorial Research Fund/Chemistry Department, Durham University, for financial support (to PKM), Johnson Matthey plc. for their generous loan of platinum salts, and A.M. Kenwright, C.F. Heffernan and I. McKeag for their assistance in recording some of the NMR spectra.

References

[1] C. Claver, E. Fernandez, A. Gillon, K. Heslop, D.J. Hyett, A. Martorell, A.G. Orpen, P.G. Pringle, Chem. Commun. (2000) 961.
[2] M. Weis, C. Waloch, W. Seiche, B. Breit, J. Am. Chem. Soc. 1258 (2006) 4188.
[3] Y. Fu, G.-H. Hou, J.-H. Xie, L. Xing, L.-X. Wang, Q.-L. Zhou, J. Org. Chem. 69 (2004) 8157.
[4] G.-H. Hou, J.-H. Xie, L.-X. Wang, Q.-L. Zhou, J. Am. Chem. Soc. 128 (2006) 11774.
[5] M.T. Reetz, A. Gosberg, R. Goddard, S.-H. Kyung, Chem. Commun. (1998) 2077.
[6] M.T. Reetz, T. Sell, Tetrahedron Lett. 41 (2000) 6333.
[7] D.W. Norman, C.A. Carraz, D.J. Hyett, P.G. Pringle, J.B. Sweeney, A.G. Orpen, H. Phetmung, R. Wingard, J. Am. Chem. Soc. 130 (2008) 6840.
[8] R. van Duren, L.L.J.M. Cornelissen, J.I. Van der Vlugt, J.P.J. Huijbers, A.M. Mills, A.L. Spek, C. Müller, D. Vogt, Helv. Chim. Acta 89 (2006) 1547.
[9] L. Dahlenburg, S. Mertel, J. Organomet. Chem. 630 (2001) 221.
[10] R.D. Chambers, K.B. Dillon, T.A. Straw, J. Fluorine Chem. 56 (1992) 385.
[11] M. Freytag, J. Grunenberg, P.G. Jones, R. Schmutzler, Z. Anorg. Allg. Chem. 634 (2008) 1256.
[12] A.H. Cowley, M. Pakulski, N.C. Norman, Polyhedron 6 (1987) 915.
[13] L. Dahlenburg, A. Kaunert, Acta Crystallogr., Sect. C 54 (1998) 1016.
[14] C. Eckert, L. Dahlenburg, A. Wolski, Z. Naturforsch., Teil B 50 (1995) 1004.
[15] A.H. Cowley, F.P. Gabbaï, S. Corbelin, A. Decken, Inorg. Chem. 34 (1995) 5931.
[16] X. Chen, R.C. Smith, J.D. Protasiewicz, Chem. Commun. (2004) 146.
[17] M. Freytag, P.G. Jones, R. Schmutzler, M. Yoshifuji, Heteroat. Chem. 12 (2001) 300.
[18] J. Krill, I.V. Shevchenko, A. Fischer, P.G. Jones, R. Schmutzler, Chem. Ber. 130 (1997) 1479.
[19] V. Plack, J.R. Goerlich, H. Thönnessen, P.G. Jones, R. Schmutzler, Heteroat. Chem. 10 (1999) 277.
[20] A. Pidcock, R.E. Richards, L.M. Venanzi, J. Chem. Soc. (A) (1966) 1707.
[21] S.O. Grim, R.L. Keiter, W. McFarlane, Inorg. Chem. 6 (1967) 1133.
[22] K.B. Dillon, A.E. Goeta, J.A.K. Howard, P.K. Monks, H.J. Shepherd, in preparation.
[23] R.J. Puddephatt, P.J. Thompson, J. Chem. Soc., Dalton Trans. (1975) 1810.
[24] R.J. Puddephatt, P.J. Thompson, J. Organomet. Chem. 120 (1976) C51.
[25] R.J. Puddephatt, P.J. Thompson, J. Chem. Soc., Dalton Trans. (1977) 1219.
[26] E. Matern, J. Pikies, G. Fritz, Z. Anorg. Allg. Chem. 626 (2000) 2136.
[27] S. Otto, A.J. Muller, Acta Crystallogr., Sect. C 57 (2001) 1405.
[28] G.G. Messmer, E.L. Amma, Inorg. Chem. 5 (1966) 1775.
[29] D.F. Mullica, J.D. Oliver, D.A. Grossie, Acta Crystallogr., Sect. C 43 (1987) 591.
[30] H. Kin-Chee, G.M. McLaughlin, M. McPartlin, G.B. Robertson, Acta Crystallogr., Sect. B 38 (1982) 421.
[31] J.P.H. Charmant, C. Fan, N.C. Norman, P.G. Pringle, Dalton Trans. (2007) 114.
[32] M.A. Bennett, H.-K. Chee, G.B. Robertson, Inorg. Chem. 18 (1979) 1061.
[33] D.K. Wicht, D.S. Glueck, L.M. Liable-Sands, A.L. Rheingold, Organometallics 18 (1999) 5130.
[34] M.A. Bennett, K.-C. Ho, J.C. Jeffery, G.M. McLaughlin, G.B. Robertson, Aust. J. Chem. 35 (1982) 1311.
[35] G.G. Mather, A. Pidcock, G.J.N. Rapsey, J. Chem. Soc., Dalton Trans. (1973) 2095.
[36] R.J. Blau, J.H. Espenson, Inorg. Chem. 25 (1986) 878.
[37] A. Crispini, K.N. Harrison, A.G. Orpen, P.G. Pringle, J.R. Wheatcroft, J. Chem. Soc., Dalton Trans. (1996) 1069.
[38] R.J. Gillespie, Coord. Chem. Rev. 197 (2000) 51.
[39] A.M.Z. Slawin, P.G. Waddell, J.D. Woollins, Acta Crystallogr., Sect. E 63 (2007) m2017.
[40] L. Dahlenburg, C. Becker, J. Höck, S. Mertel, J. Organomet. Chem. 564 (1998) 155.
[41] J.I. van der Vlugt, R. Sablong, A.M. Mills, H. Kooijman, A.L. Spek, A. Meetsma, D. Vogt, Dalton Trans. (2003) 4690.
[42] M.J. Atherton, J. Fawcett, A.P. Hill, J.H. Holloway, E.G. Hope, D.R. Russell, G.C. Saunders, R.M.J. Stead, J. Chem. Soc., Dalton Trans. (1997) 1137.
[43] F.H. Allen, Acta Crystallogr., Sect. B 58 (2002) 380 (CCDC, February 2009 distribution).
[44] W. Baratta, P.S. Pregosin, Inorg. Chim. Acta 209 (1993) 85.
[45] N.M. Boag, M.S. Ravetz, J. Chem. Soc., Dalton Trans. (1995) 3473.
[46] S.M.M. Cornet, K.B. Dillon, A.E. Goeta, A.L. Thompson, Acta Crystallogr., Sect. C 61 (2005) m74.
[47] J. Cosier, A.M. Glazer, J. Appl. Crystallogr. 19 (1986) 105.
[48] SMART-NT, Data Collection Software, version 6.1, Bruker Analytical X-ray Instruments Inc., Madison, WI, USA, 2000.
[49] SAINT-NT, Data Reduction Software, version 6.1, Bruker Analytical X-ray Instruments Inc., Madison, WI, USA, 2000.
[50] O.V. Dolomanov, L.J. Bourhis, R.J. Gildea, J.A.K. Howard, H. Puschmann, J. Appl. Crystallogr. 42 (2009) 339.
[51] G.M. Sheldrick, Acta Crystallogr., Sect. A 64 (2008) 112.